MOLECULAR AND CELLULAR BIOLOGY, July 2008, p. 4629–4641 Vol. 28, No. 14
0270-7306/08/$08.00+0 doi:10.1128/MCB.00120-08

Nuclear Factor 45 (NF45) Is a Regulatory Subunit of Complexes with NF90/110 Involved in Mitotic Control▽†

Deyu Guan,[1] Nihal Altan-Bonnet,[3] Andrew M. Parrott,[1] Cindy J. Arrigo,[1]‡ Quan Li,[1] Mohammed Khaleduzzaman,[1]§ Hong Li,[1] Chee-Gun Lee,[1] Tsafi Pe'ery,[1,2] and Michael B. Mathews[1]*

Departments of Biochemistry and Molecular Biology[1] and Medicine,[2] New Jersey Medical School, University of Medicine and Dentistry of New Jersey, 185 South Orange Avenue, P.O. Box 1709, Newark, New Jersey 07103-1709, and Department of Biological Sciences, Rutgers University, Newark, New Jersey 07102[3]

Received 22 January 2008/Returned for modification 29 February 2008/Accepted 28 April 2008

Nuclear factor 90 (NF90) and its C-terminally extended isoform, NF110, have been isolated as DNA- and RNA-binding proteins together with the less-studied protein NF45. These complexes have been implicated in gene regulation, but little is known about their cellular roles and whether they are redundant or functionally distinct. We show that heterodimeric core complexes, NF90-NF45 and NF110-NF45, exist within larger complexes that are more labile and contain multiple NF90/110 isoforms and additional proteins. Depletion of the NF45 subunit by RNA interference is accompanied by a dramatic decrease in the levels of NF90 and NF110. Reciprocally, depletion of NF90 but not of NF110 greatly reduces the level of NF45. Coregulation of NF90 and NF45 is a posttranscriptional phenomenon, resulting from protein destabilization in the absence of partners. Depletion of NF90-NF45 complexes retards cell growth by inhibition of DNA synthesis. Giant multinucleated cells containing nuclei attached by constrictions accumulate when either NF45 or NF90, but not NF110, is depleted. This study identified NF45 as an unstable regulatory subunit of NF90-NF45 complexes and uncovered their critical role in normal cell division. Furthermore, the study revealed that NF90 is functionally distinct from NF110 and is more important for cell growth.

Human nuclear factor 90 (NF90) and nuclear factor 45 (NF45) were originally purified as a sequence-specific DNA binding complex regulating the interleukin-2 (IL-2) promoter (10, 17). NF90 is the founder member of a family of proteins generated from differentially spliced transcripts of the *ILF3* gene (12). NF90 and NF110, which differ at their C termini, are the two most prominent *ILF3* isoforms in cells (12, 33, 42, 55). Both have been repeatedly isolated in diverse studies and have been given a variety of names. For example, MPP4 (M-phase phosphoprotein 4) is similar, if not identical, to NF90 and is phosphorylated during M phase (23), and closely related proteins 4F.1 and 4F.2 were characterized in *Xenopus* as double-stranded RNA (dsRNA)-binding proteins (3). NF90 is also known as DRBP76, NFAR1, and TCP80 (34, 43, 55), and NF110 is also known as ILF3, NFAR2, TCP110, and CBTF^{122} (4, 43, 53, 55). Underlining the importance of these proteins, knockout of the mouse *ILF3* gene led to muscle degeneration, respiratory failure, and death soon after birth (44).

NF90 and NF110 contain two dsRNA binding motifs (dsRBMs) which are responsible for their ability to interact with structured RNA. They also have an RGG domain that is capable of nucleic acid binding, and NF110 has an additional GQSY region that can interact with nucleic acids. Although characterized as DNA-binding proteins (17, 36, 40, 41), NF90 and NF45 do not contain a recognized sequence-specific DNA-binding domain and the complex containing NF90 and NF45 does not appear to interact with DNA directly. NF90 and NF45 have been purified in complexes containing the Ku proteins and DNA-protein kinase (PK), as well as eukaryotic initiation factor 2 (eIF2), and it is likely that their interactions with DNA are mediated by Ku or DNA-PK (5, 50).

On the other hand, the direct binding of NF90 and its relatives to double-stranded and structured single-stranded RNA has been well studied (22, 33, 37) and much of the functional research on NF90 and NF110 is based on their RNA binding properties. NF90 and NF110 (as well as NF45) are mainly located in the nucleus through binding to RNA as well as to protein (33). The two dsRBMs in NF90 and NF110 are required for their activity in regulating gene expression (38), and dsRBM mutations that interfere with RNA binding reduce the stimulation of gene expression by NF110 (37). NF90 forms complexes with a number of small noncoding RNAs (31, 32) as well as mRNAs. In activated Jurkat cells, NF90 is exported from the nucleus to the cytoplasm, binds to ARE elements in the 3′ untranscribed region of IL-2 mRNA and stabilizes the mRNA (45). Similarly, NF90 binds to the 3′ untranscribed region of MyoD and p21$^{WAF1/CIP1}$ mRNAs and is implicated in stabilizing these mRNAs (44). Genetic ablation of NF90 in mice led to rapid degradation of MyoD and p21$^{WAF1/CIP1}$ mRNAs. NF90 also binds several viral RNAs (16, 22, 26, 27, 46), and a C-terminal variant of NF90 (NF90ctv or NF90c) attenuates human immunodeficiency virus type 1 replication in a stably transduced cell line. These observations suggest that

* Corresponding author. Mailing address: Phone: (973) 972-4411. Fax: (973) 972-5594. E-mail: mathews@umdnj.edu.
‡ Present address: Department of Biology, New Jersey City University, Jersey City, NJ 07002.
§ Department of Pathobiological Sciences, School of Veterinary Medicine, Louisiana State University, Baton Rouge, LA 70803.
† Supplemental material for this article may be found at http://mcb.asm.org/.
▽ Published ahead of print on 5 May 2008.

NF90 is exploited during virus multiplication in mammalian cells. It is interesting that NF90 interacts and cofractionates with the eIF2 kinase protein kinase R (PKR), as well as with eIF2, and is a substrate for phosphorylation by PKR (19, 29, 30, 34, 50).

The properties of NF45 are less well understood, and its specific function is unknown. NF45 is encoded by the *ILF2* gene. In mice, NF45 is expressed at high levels in brain, kidney, and testis (56), all of which also contain high levels of NF90 and/or NF110 (44), although their distributions in some other tissues do not appear to match. NF45 is complexed with NF90 in many cell lines and in human placenta (16, 17, 22, 27, 28, 41, 46, 50). In the HTB-14 glioma cell line, however, NF90 and NF45 were largely distributed in different fractions with little overlap in size exclusion chromatography (27). The N-terminal regions of both NF90/110 and NF45 contain DZF (dsRBM- and zinc finger associated) motifs which are shared with the conserved protein ZFR that is important for development of flies and mice (25). Overexpression of NF45 enhanced the stimulation of cytomegalovirus promoter by NF90 (38). In yeast (*Saccharomyces cerevisiae*), NF45 inhibited PKR, whereas NF90 activated this kinase (30).

It is not clear whether the cellular roles of NF90 and NF110 are identical or distinct and whether NF45, NF90, and NF110 function in cells as monomers or as complexes. We characterized complexes containing these proteins and used RNA interference to elucidate their function. NF90 and NF110 form heterodimeric core complexes with NF45 and large in vivo complexes in which multiple NF90/110 isoforms interact with each other and with additional proteins. Depletion of NF45 led to decreased levels of NF90 and NF110. This coregulation is at the protein level: the stability of NF90 family proteins is dependent on binding to their NF45 partner. Most interestingly, cell growth is retarded and giant multinucleated cells accumulate when the expression of NF45 or NF90, but not NF110, is reduced in HeLa cells.

MATERIALS AND METHODS

Cell lines and plasmids. HeLa S3 and HEK 293 cells were cultured in Dulbecco's modified Eagle's medium (DMEM) (Mediatech, Inc.). 293 cell lines expressing NF90b or NF110b or empty vector were reported previously (33). Cells cultured in six-well plates (8×10^4/well) were transfected 24 h after seeding using Lipofectamine 2000 (2 μl; Invitrogen). The reagent was incubated with 1 μg plasmid DNA or 80 pmol small interfering RNA (siRNA) in 100 μl DMEM for 15 min at room temperature. Expression vectors pcDNA-NF45, pcDNA-NF90a, pcDNA-NF90b, pcDNA-NF110a, pcDNA-NF110b, and pcDNA-GFP-NF90c have been reported elsewhere (37–39).

RNA interference. The siRNA oligonucleotides C, D2, D3, D4, and D5 (Dharmacon) were used at a final concentration of 25 nM, except where noted otherwise. Plasmids d2, d3, d4, and d5, expressing short hairpin RNA (shRNA) corresponding to D2, D3, D4, and D5 and a control hairpin RNA containing a mismatch sequence (c; 5′ half from D2 and 3′ half from D4) were constructed according to the two-step method (48). Synthetic DNA sequences encoding shRNA was inserted between the ApaI and EcoRI sites of pSilencer 1.0-U6 (Ambion). The KpnI-EcoRI fragments from the resultant plasmids were inserted into pcDNA3.1. To generate stable cell lines, HeLa cells were transfected with these plasmids and G418 (GIBCO) was added to the medium to a final concentration of 1 μg/ml at 24 h posttransfection. Resistant cells were clonally selected 10 to 14 days later, screened by immunoblotting, and cryopreserved. Cultures were maintained in the presence of G418 for up to 10 passages.

Glycerol gradient analysis. Cytoplasmic and nuclear extracts (90 μl each) from 293 cells (33) were incubated for 30 min at 37°C in the absence or presence of RNases A and T_1 (0.01 and 0.5 U/μl, respectively) and then loaded onto 10 to 40% glycerol gradients in polysome extraction buffer (15 mM Tris-HCl [pH 7.4], 15 mM $MgCl_2$, 200 mM NaCl, 100 μg/ml cycloheximide, 2 μg/ml leupeptin, 2 μg/ml aprotinin, 1 mM dithiothreitol) and centrifuged at 150,000 × *g* for 20 h at 4°C in an SW41 rotor (Beckman). Fractions (25 × 200 μl) were removed by aspiration. Proteins were resolved in 7.5% sodium dodecyl sulfate (SDS)–polyacrylamide gels and analyzed by immunoblotting. A gradient containing protein standards (50 μg bovine serum albumin, 100 μg aldolase, and 100 μg catalase) was centrifuged simultaneously, and fractions were analyzed by A_{280} and gel electrophoresis followed by staining.

Gel filtration chromatography. A 10-ml Sephacryl S-400 HR column (Amersham Biosciences) was equilibrated with running buffer (50 mM Tris-HCl [pH 8.0], 150 mM NaCl, 0.1 mM EDTA). Cytoplasmic and nuclear extracts of 293 cells were loaded, and 30 100-μl fractions were collected. The column was calibrated with Bio-Rad standards as follows (molecular mass, Stokes radius): thyroglobulin (670 kDa, 8.5 nm), bovine gammaglobulin (158 kDa, 5.34 nm), chicken ovalbumin (44 kDa, 3.05 nm), equine myoglobin (17 kDa, 2.05 nm), and vitamin B_{12} (1.35 kDa, 0.16 nm). Proteins were detected by A_{280} and gel electrophoresis followed by staining. Vitamin B_{12} was detected by A_{361}.

Immunoblotting and immunoprecipitation. Cells were harvested by scraping. Subsequent procedures were carried out at 4°C except as noted. Lysates in IP (immunoprecipitation) buffer (50 mM Tris-HCl [pH 7.4], 150 mM NaCl, 1 mM EDTA, 1% Triton X-100, 2 μg/ml leupeptin, 2 μg/ml aprotinin, 1 mM dithiothreitol) were clarified at 12,000 rpm for 10 min, and 10 to 20 μg protein was loaded onto 7.5% SDS–polyacrylamide gels. Immunoblots were probed with antibody against NF90 (rabbit, 1:100) (33), NF45 (rabbit, 1:200) (33), DRBP76 (mouse, 1:1,000; BD Transduction Laboratories), or actin (mouse, 1:2,000; Sigma) or with Omni-tag monoclonal antibody (mouse, 1:5,000; Santa Cruz). Note that anti-NF90 and anti-DRBP76 both react with NF110. For immunoprecipitation, anti-NF90 (1:25), anti-NF45 (1:50), or anti-Omni-tag (1:500) antibody was mixed with 10 μl protein A-Sepharose beads (Amersham Biosciences) for 2 h. The beads were washed three times with IP buffer, mixed overnight with 100 μl supernatant of cell extract, and then washed three times in IP buffer. Proteins were resolved in 7.5% SDS–polyacrylamide gels and analyzed by autoradiography or immunoblotting.

GST pull-down assays. Glutathione *S*-transferase (GST) and GST fusion proteins were produced and used in pull-down assays as described previously (29). Radiolabeled proteins were synthesized in wheat germ (Promega TnT) with [^{35}S]methionine from linearized plasmids encoding NF90, NF110, and NF45 or their mutants. Plasmids used to produce truncated proteins were made by digestion of parental vectors at appropriate sites with restriction enzymes or by inserting PCR fragments into pcDNA-3.1.

Metabolic labeling. For thymidine incorporation experiments, cells were seeded in 12-well plates at 4×10^4/well. At 48 h after transfection (HeLa cells) or seeding (cell lines expressing shRNAs), cells were labeled with 0.5 μCi [^{3}H]thymidine/well for 1 h and then washed three times with phosphate-buffered saline (PBS). Samples of trichloroacetic acid precipitates were dissolved in 0.1 N NaOH and mixed with Ecolite for liquid scintillation counting. For protein labeling, HeLa cells (2×10^5/well in six-well plate) were transfected with siRNA. At 48 h posttransfection, cells were washed twice with PBS and medium was changed to GIBCO methionine-negative DMEM containing 10% fetal bovine serum and 50 μCi [^{35}S]methionine. Cells were cultured for 1 h and harvested for production of cell extracts. For "chase" incubations, the medium was removed, the cells were washed three times with PBS, and methionine-positive medium containing 10% fetal bovine serum was added. Incubation was resumed, and cells were harvested at hourly intervals.

Immunofluorescence and live-cell imaging. Cells expressing shRNAs cultured on coverslips were washed once with PBS and fixed in freshly made PBS containing 4% paraformaldehyde for 10 min at room temperature. After three washes with PBS, the cells were permeabilized in PBS containing 0.2% Triton X-100 for 5 min. After washing three times in PBS, the cells were blocked with 5% donkey serum in PBS containing 0.2% Triton X-100 at room temperature for 1 h. Antitubulin antibody (Sigma) was added in blocking buffer (PBS containing 0.2% Triton X-100 and 5% donkey serum) at 1:1,000 (vol/vol) and allowed to react at 4°C overnight. Secondary antibody (donkey anti-mouse antibody; Jackson ImmunoResearch Laboratories, Inc.) was added at 1:800 (vol/vol), and incubation continued at room temperature for 1 h. Hoechst 33342 was included with the secondary antibody at 100 μg/ml. Cells were observed by fluorescent microscopy using an oil immersion lens (60 × 10). To observe multinucleated cells, the d5 cell line cultured in a two-well chambered coverglass (Nunc) was transfected with 1 μg pEGFP-N1 (Clontech Laboratory, Inc.) or histone 2B-cyan fluorescent protein (histone-CFP) (1). At 48 h after transfection, cells were observed by confocal microscopy (Zeiss LSM 510 META). Photobleaching was done as described previously (1).

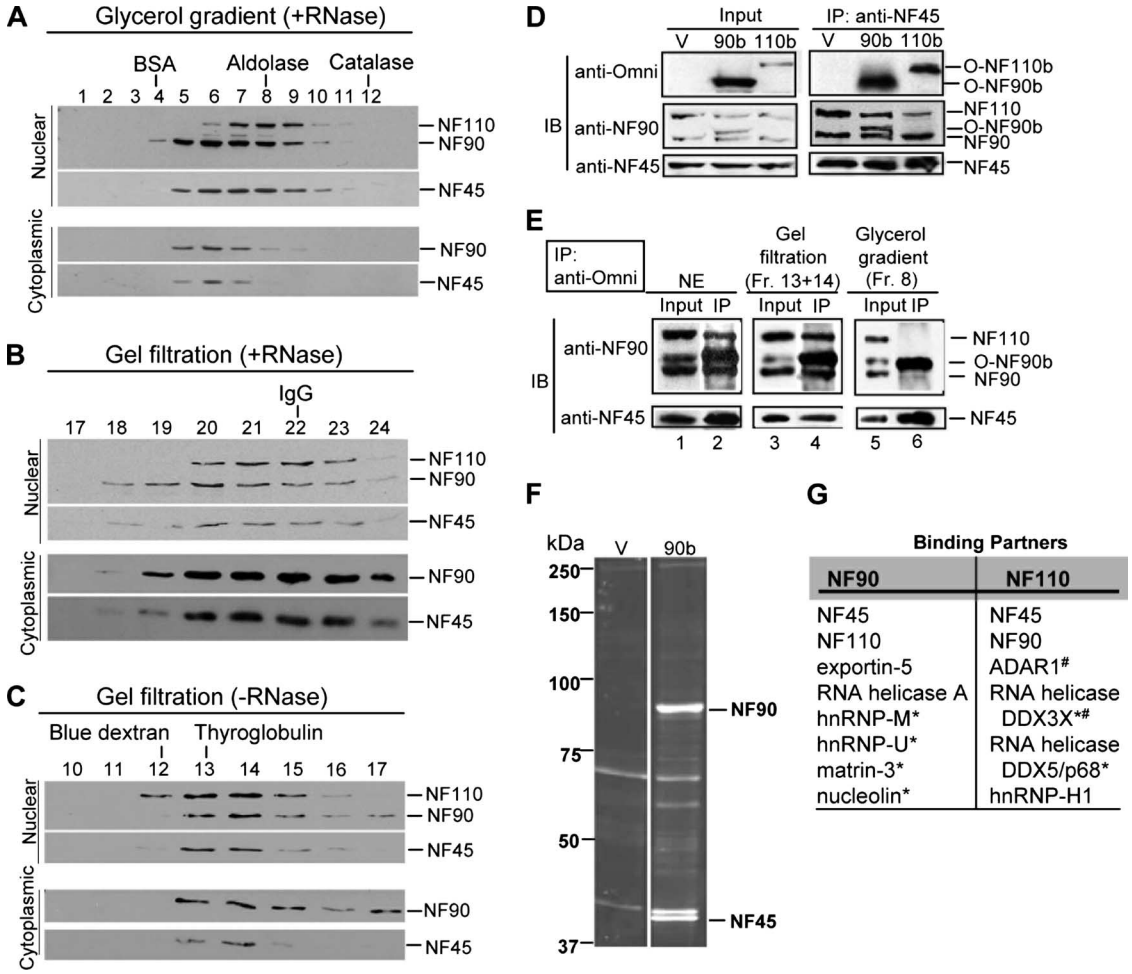

FIG. 1. Analysis of NF45, NF90, and NF110 complexes in cells. (A) Glycerol gradient fractionation of nuclear and cytoplasmic extracts of 293 cells. After sedimentation, all fractions were analyzed by immunoblotting with anti-NF90 and anti-NF45 antibodies. Fraction numbers and the positions of protein standards are indicated. Nonreactive regions of the gradient are not shown. Indistinguishable results were obtained with RNase-treated extracts (not shown). BSA, bovine serum albumin. (B and C) Gel filtration chromatography of nuclear and cytoplasmic extracts of 293 cells after (B) or without (C) RNase treatment. Proteins were analyzed as in panel A. IgG, immunoglobulin G. (D) Coimmunoprecipitation results. Immunoprecipitates (IP) were prepared with anti-NF45 antibody from whole-cell extract of 293 cell lines expressing Omni-NF90b or Omni-NF110b or containing empty vector (V). Immunoblots of the IP (right) and input (left) proteins were probed with anti-Omni tag, anti-NF90, and anti-NF45 antibodies. (E) IP were prepared with anti-Omni tag antibody from nuclear extract of cell lines expressing NF90b (left) and from gel filtration fraction (Fr.) 13 plus 14 (middle) or glycerol gradient fraction 8 (right) prepared from this extract. Immunoblots (IB) of the IP and input proteins were probed with anti-DRBP76 and anti-NF45 antibodies. (F and G) Proteins associated with NF90/110. Cellular complexes were immunoaffinity isolated from control (V) and Omni-NF90b (90b) cell lines and resolved by SDS gel electrophoresis. Purified proteins were stained with SYPRO Ruby and visualized with a UV transilluminator: a representative gel is shown. Proteins in Omni-NF90b or Omni-NF110b complexes were identified by matrix-assisted laser desorption–time of flight mass spectrometry. The proteins and numbers of peptides identified for each protein are listed. *, novel NF90/110-associated proteins; #, found only in complexes from extracts that were not treated with RNase.

RESULTS

Heterodimeric core complexes between NF45 and NF90 or NF110. Evidence that NF45 associates with NF90 in a variety of human cells and tissues includes their copurification through conventional (17, 46, 50) and RNA affinity chromatography (16, 22, 26) and coimmunoprecipitation (27–29, 38, 41). Although less extensively documented, similar observations have been made for NF45-NF110 interactions (16, 28, 29, 41, 50). The molecular weights and stoichiometries of these complexes have not been rigorously determined, however. To characterize the complexes, we used a method that allows molecular weight to be determined without assumptions about molecular shape (47). This method requires the independent measurement of sedimentation coefficient (e.g., by gradient sedimentation) and Stokes radius (e.g., by gel filtration). In HeLa and 293 cells, NF90 is distributed between the nuclear and cytoplasmic fractions while NF110 is almost exclusively nuclear (33). Because the great majority of NF90 and NF110 is complexed with RNA (33), we treated nuclear and cytoplasmic extracts with RNase prior to fractionation: complete digestion of RNA was monitored by gel analysis (data not shown). NF90 and NF110 sedimented through glycerol gradients at approximately 5.9S and 7.7S, respectively (Fig. 1A), and gel filtration results (Fig. 1B) gave estimates of 4.7 nm and 4.2 nm for their

Stokes radii. Similar gel filtration behavior for NF90 was observed in a previous study (27). In both types of fractionation, all of the NF45 cosedimented with NF90 and NF110, indicating that these proteins are predominantly complexed together in cells. Combining the data with the Siegel and Monty equation yields molecular masses of 114 kDa for the NF90-containing complex and 135 kDa for the NF110-containing complex, in close agreement with those calculated for 1:1 complexes (119 kDa for NF90-NF45 and 138.5 kDa for NF110-NF45). We conclude that both complexes are heterodimeric as previously assumed, and that their interaction is RNA independent. Estimates of the frictional coefficient, f/f_0, gave values of 1.39 for NF90 and 1.33 for NF110, implying that the complexes are not highly asymmetrical (14, 47).

Higher-order complexes in cells. When RNase pretreatment was omitted, all three proteins eluted from gel filtration in earlier fractions and a small proportion of the NF110 was excluded from the column (Fig. 1C), consistent with their presence in much larger complexes. Omitting RNase pretreatment did not affect their distribution in glycerol gradients, however (not shown). When a fraction (fraction 8) from glycerol gradient analysis performed without RNase treatment was subjected to gel filtration, the proteins were all detected in fractions 20 to 24, indicating that the large RNA-dependent complexes are not stable in glycerol gradient conditions (data not shown). Without their sedimentation coefficients, we were unable to calculate the molecular weights of these large complexes by the Siegel and Monty method. From size exclusion data alone, we estimate that NF90 and NF110 are present in RNase-sensitive complexes of ~600 kDa. Similar results were obtained in HeLa cells (data not shown).

We used stable cell lines expressing Omni-tagged forms of NF90 or NF110 (33) to examine the composition of the large complexes. To verify that the exogenous tagged proteins participate in complex formation with NF45, we first probed anti-NF45 immunoprecipitates with antibody directed against the Omni tag (Fig. 1D, right panel). Omni-NF90b and Omni-NF110b were immunoprecipitated with NF45 from the NF90b and NF110b cell lines, respectively, but not from the control cell line carrying empty vector (top panel). Probing with anti-NF90/110 antibody (middle panel) revealed the presence of endogenous NF90 and NF110 in all of the NF45 immunoprecipitates, as well as the Omni-tagged forms in those from the NF90b and NF110b cell lines (although Omni-NF110b was difficult to detect because of its weak expression in the cell line, coupled with the inefficient extraction of NF110 from nuclei). Next, we conducted reciprocal experiments to examine anti-Omni immunoprecipitates from NF90b cell extracts. Strikingly, immunoblotting with anti-NF90/110 showed that Omni-NF90b coimmunoprecipitated with the endogenous NF90 and NF110 isoforms (Fig. 1E, lane 2, top panel) as well as with NF45 (bottom panel). Similar results were obtained with the Omni-NF110b (data not shown), suggesting that the large complexes obtained by gel filtration contain multiple NF90/110 proteins. Consistent with this interpretation, endogenous NF90 and NF110 coprecipitated with Omni-NF90b from high-molecular-weight gel filtration fractions from the NF90b cell line (Fig. 1E, lane 4). Such coprecipitation was not observed from low-molecular-weight gel filtration fractions (data not shown) or from glycerol gradient fractions from the NF90b cell line (Fig. 1E, lane 6). Thus, the large complexes contain additional molecules of NF90/110, possibly interacting with each other as well as with NF45 and other proteins.

To identify further components of the large complexes, we isolated NF90 complexes from NF90b cells by affinity purification using anti-Omni antibody cross-linked to beads. Separation in SDS-polyacrylamide gels revealed the presence of many additional proteins in submolar yield relative to NF90 and NF45 (Fig. 1F). The banding patterns obtained with Omni-NF110b were similar but not identical. Individual bands were analyzed by mass spectrometry, and several proteins were identified (Fig. 1G and see Table S1 in the supplemental material). As expected, endogenous NF110 was present in Omni-NF90b immunoprecipitates and endogenous NF90 was present in Omni-NF110b immunoprecipitates. NF45 was common to NF90 and NF110 complexes, but other partners were distinct. Some of the interactions have been reported previously, with RNA helicase A, exportin-5, and ADAR-1, while novel associations were detected with hnRNP proteins, additional ATP-dependent RNA helicases (DDX3X and DDX5/p68), and proteins associated with cell structure and gene regulation (matrin-3 and nucleolin). Interestingly, hnRNP U and NF90 are both associated with 7SK complexes (52), consistent with our finding of 7SK in cross-linked complexes with NF90 (32). Most of the proteins' binding partners were observed in complexes derived from RNase-treated extracts, implying protein-protein interactions. Two exceptions were ADAR-1 and DDX3X (see Table S1 in the supplemental material).

Interactions among NF90, NF110, and NF45 in vitro. Reconstitution experiments showed that NF90c and NF45, synthesized in bacteria or a heterologous cell-free system, are able to associate in vitro (29, 30). However, NF90c was not found in cells (18, 39) and it differs at its C terminus from authentic NF90 and NF110, both of which occur in a and b isoforms distinguished by the absence or presence, respectively, of a four-amino-acid (aa) insert between their dsRBMs. To determine whether the NF90/110 isoforms all interact with NF45 in vitro, we produced them in wheat germ and conducted GST pull-down assays. Both NF110 isoforms and all three NF90 isoforms bound tightly to GST-NF45 in vitro (Fig. 2A). Quantitation indicated that the a and b isoforms of NF90 and NF110 bound at least threefold more efficiently than NF90c (data not shown), suggesting that the complex is stabilized by the natural C termini of the a and b isoforms of NF90 and NF110 or destabilized by the acidic C terminus of NF90c.

Because the large complexes in cell extracts contain two or more molecules of NF90/110, we considered the possibility that members of this protein family can interact directly with one another. In GST pull-down experiments, GST-NF90b bound to the a and b isoforms of both NF90 and NF110 (Fig. 2B), consistent with the results of yeast two-hybrid experiments (49). The N-terminal 335 residues were not required for binding, but C-terminal truncations infringing on or removing the dsRBMs were deleterious. Further experiments showed that NF90 fragments 1 to 591 and 336 to 591 retained binding activity (data not shown), mapping the region responsible to the central part of the molecule containing its two dsRBMs (Fig. 2D). Binding was resistant to treatment with RNase or high salt concentrations (up to 750 mM NaCl). Thus, as with interactions between NF90 and PKR (29) the binding of NF90

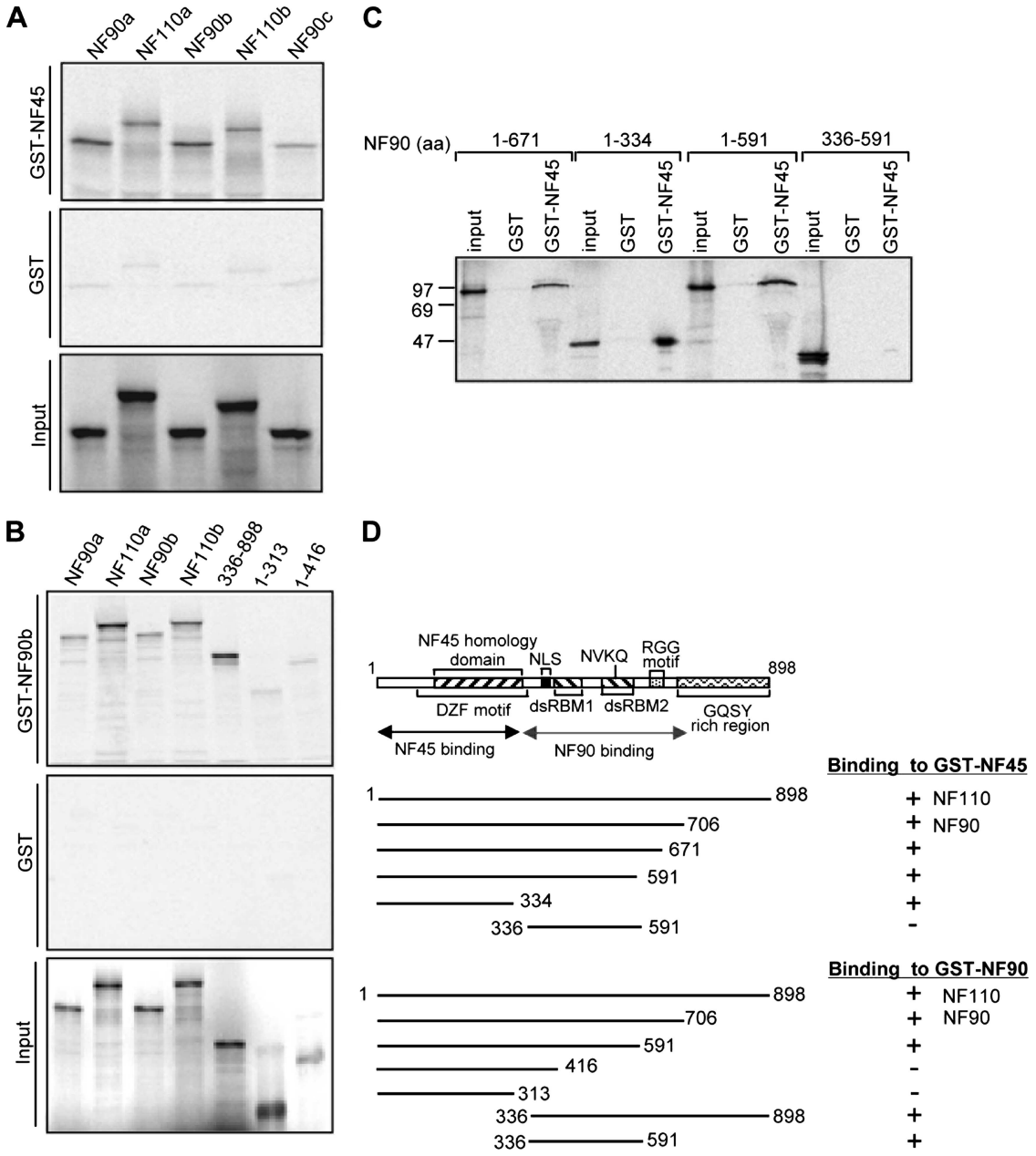

FIG. 2. Binding of NF45, NF90, and NF110 in vitro. (A) Interaction of NF90 and NF110 isoforms with GST-NF45. Equal amounts of the indicated ^{35}S-labeled proteins expressed in wheat germ (bottom panel) were bound to beads carrying GST-NF45 (top panel) or GST alone (middle panel). Bound proteins were resolved in SDS-polyacrylamide gels and analyzed by autoradiography. (B) Interaction of full-length and truncated forms of NF90 and NF110 with GST-NF90b. Experiments were conducted as in panel A. (C) Interaction of full-length and truncated forms of NF90 with GST-NF45. Experiments were conducted as in panel A. (D) Summary of pull-down assays mapping the binding sites for NF45 and NF90 on NF90/110.

with NF90 and NF110 is mediated by the proteins' dsRBMs but is not dependent on RNA.

Immunoprecipitation experiments showed that the N-terminal region (aa 1 to 418) of NF90/110 binds strongly to NF45, whereas the C-terminal region (aa 403 to 670) displayed a weak interaction that could be indirect (38). To examine the interactions in vitro, we used GST-NF45 to pull down fragments of NF90. The results (Fig. 2C and D) demonstrated the existence of a strong site for NF45 binding between aa 1 and 334 of NF90/110. Little or no binding was observed with aa 336 to 591. These findings are consistent with direct binding of NF45 to the N-terminal region of NF90/110 containing the DZF domain and weaker indirect binding in vivo to the RNA-binding domain mediated by interactions between NF90 isoforms.

Previous GST pull-down assays gave no evidence of homomeric NF45-NF45 interactions (29). Therefore, taken together, our results suggest that NF90/110 interacts directly via

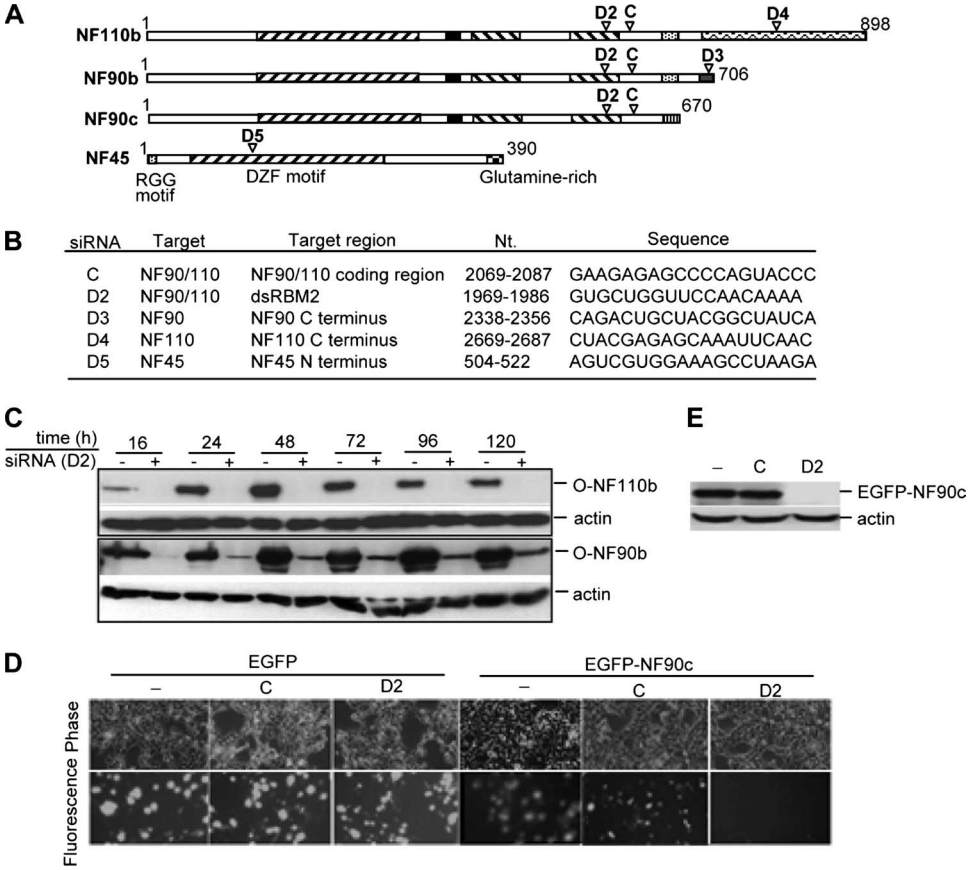

FIG. 3. Effect of siRNA on expression of ectopic NF90 and NF110. (A) Schematic of NF110, NF90, and NF45 showing regions targeted by siRNAs C, D2, D3, D4, and D5. Note that the NF90a and NF110a isoforms are identical to NF90b and NF110b, respectively, except for the NVKQ sequence lacking in the a isoforms. (B) Sequence and targets of siRNAs. (C) Time course of inhibition by D2 siRNA. 293 cells were transfected with 25 nM siRNA together with 2 μg pcDNA-NF90b or pcDNA-NF110b. Cells were harvested at the times indicated and analyzed by immunoblotting with anti-Omni tag and antiactin antibodies. (D) Specificity of D2 siRNA. 293 cells were transfected with pcDNA-EGFP or pcDNA-EGFP-NF90c together with siRNA C or D2 or without siRNA (−). At 48 h after transfection, cells were observed by phase-contrast and fluorescence microscopy. (E) Cells transfected with pcDNA-EGFP-NF90c were harvested, and extracts were examined by immunoblotting using anti-NF90 and antiactin antibodies.

its N-terminal region with NF45 to form heterodimeric complexes. Furthermore, homomeric NF90/110 interactions via its dsRBMs may contribute to the formation of higher-order complexes.

Coregulation of NF90 and NF45. We designed a series of siRNAs to evaluate the biological effects of knocking down NF45 and members of the NF90 family, individually or collectively (Fig. 3A and B). D2 is directed against both NF90 and NF110, whereas D3, D4, and D5 selectively target NF90, NF110, and NF45, respectively. Although designed to knock down NF90 and NF110, RNA C was ineffective and served as a control. To optimize NF90 depletion, we cotransfected 293 cells with D2 and a vector expressing Omni-NF90b. Increasing concentrations of D2 siRNA progressively reduced NF90b accumulation, and it was >90% effective at 25 nM (see Fig. S2 in the supplemental material). Higher concentrations did not result in more complete knockdown, and RNA C was ineffective even at high concentrations (data not shown). D2 effectively depleted tagged NF110b as well as NF90b (Fig. 3C). Its silencing action was observed as early as 16 h after transfection and persisted for as long as 120 h, although synthesis gradually broke through the inhibition. To verify the specificity of knockdown, cells were cotransfected with siRNA and plasmids expressing enhanced green fluorescent protein (EGFP)-NF90c or EGFP alone. D2 silenced EGFP-NF90c expression, while C was ineffective (Fig. 3D), in keeping with immunoblotting results (Fig. 3E). Neither siRNA had any effect on EGFP fluorescence. From our observations, it would appear that the residual expression of exogenous NF90b that is resistant to knockdown by D2 comes from a low level of expression of NF90b in a large number of cells rather than from a few cells that are wholly resistant.

Similarly, endogenous NF90 and NF110 were both silenced by D2 siRNA (Fig. 4A), albeit somewhat less efficiently than the exogenous proteins. As expected, siRNAs D3 and D4, directed at specific sequences in the proteins' C termini, selectively depleted endogenous NF90 and NF110, respectively. Likewise, D5 siRNA silenced the expression of endogenous NF45. Remarkably, we observed additional inhibitory effects. In particular, D2 and D3 (specific for NF90 and NF90/110) also brought down the level of NF45. Conversely, D5 (specific for NF45) also brought down the levels of both NF90 and

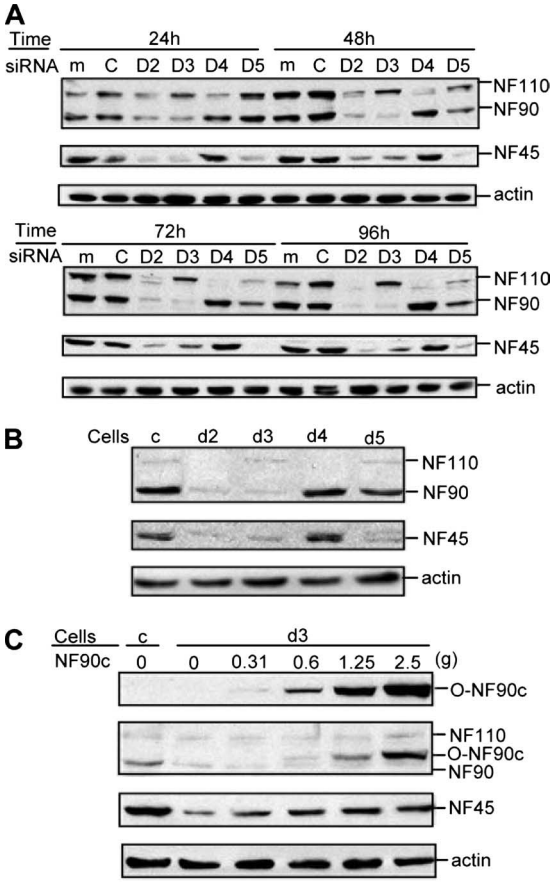

FIG. 4. Knockdown of endogenous NF45, NF90, and NF110. (A) Transient expression of siRNA. HeLa cells were mock transfected (m) or transfected with control (C), D2, D3, D4, or D5 siRNA. At the times indicated, cells were harvested and analyzed by immunoblotting with antibodies against NF90, NF45, and actin. (B) Cell lines expressing shRNAs. Cells from the stable cell lines c, d2, d3, d4, and d5 were examined as in panel A. (C) Rescue of NF45 expression by ectopic NF90c. Cells of the d3 cell line were transfected with increasing concentrations of pcDNA-NF90c, using pcDNA3.1 empty vector to maintain a constant amount of transfected DNA. Cells were harvested at 48 h after transfection for immunoblotting analysis as in panel A.

NF110 (Fig. 4A). However, D4 (specific for NF110) elicited little or no decrease in NF45. It is notable that when NF45 was targeted by D5 siRNA, the level of NF45 protein fell rapidly (by 24 h) and the levels of NF90 and NF110 declined relatively slowly (visible after 48 h). This cross-inhibition did not extend to proteins such as actin (Fig. 3 and 4), EGFP (Fig. 4), tubulin, or nucleolin (data not shown). The mutual regulation observed between NF90/110 and NF45 is consistent with a secondary effect due to complex formation.

We further evaluated the specificity of the cross-inhibition in cell lines that stably express corresponding shRNAs. Cross-regulation between NF90 and NF45 was seen in the d2, d3, and d5 cell lines (corresponding to D2, D3, and D5 siRNAs, respectively), but not between NF110 and NF45 in the d4 line (corresponding to D4 in Fig. 4B). This mirrors the results of the silencing experiments (Fig. 4A). Furthermore, we conducted a rescue experiment. The d3 cell line was transfected with a vector expressing the NF90c isoform, which lacks the D3 siRNA target region at the NF90 C terminus (Fig. 3A) but contains the rest of the molecule, including the NF45 binding site (Fig. 2). Accordingly, NF90c protein accumulated in transfected d3 cells (Fig. 4C, top panel). Although the levels of endogenous NF90 and NF110 were unaffected (second panel), NF45 levels were restored by NF90c expression (third panel).

Taken together, these results indicate that the cellular concentrations of NF45 and NF90/110 are coordinately regulated, consistent with their presence in heterodimeric complexes. Exceptionally, the level of NF45 did not decline discernibly in concert with reduced levels of NF110, even though NF45 knockdown caused a reduction in NF110 level. Interestingly, expression of exogenous NF90 or NF110 did not result in substantially elevated levels of total NF90/110 or of NF45 (Fig. 1D and data not shown), suggesting that the cell has mechanisms limiting the overall concentrations of these proteins.

Mutual regulation of NF90 and NF45 is posttranslational. Although there were no obvious similarities between the NF90 and NF45 target sequences, we considered the possibility that coregulation occurs by a mechanism operating at the mRNA level. RNase protection assays were conducted with probes specific for NF45 and NF90/110 mRNAs and for glyceraldehyde-3-phosphate dehydrogenase (GAPDH) mRNA as a control. No cross-inhibition activity was observed at the RNA level (see Fig. S1 in the supplemental material). The results showed that all of the siRNAs were specific for their target mRNAs, and no effects were observed on GAPDH RNA. Thus the coregulation of NF90 and NF45 involves a process downstream of the level of mRNA concentration in the cell, probably either protein synthesis or protein stability. To distinguish between these alternatives, we first monitored the synthesis of NF90, NF110, and NF45. Cells were pulse-labeled with [^{35}S]methionine at 48 h after transfection with D3, D5, or control siRNA. Labeled proteins were immunoprecipitated with antibodies against NF90 and NF110 or against NF45, resolved by gel electrophoresis, and observed by autoradiography (Fig. 5A). D3, which targets NF90 mRNA, inhibited the synthesis of NF90 but not of NF110 or NF45. Correspondingly, D5, which targets NF45 mRNA, inhibited the synthesis of NF45 but not of NF90 or NF110. These observations match the effects on mRNA levels seen in RNase protection assays (see Fig. S1 in the supplemental material) and argue that the cross-inhibition phenomenon is not exerted at the translational level. NF45 synthesis was also unaffected by D2 and D4 siRNAs, which, respectively, target both NF90 and NF110 and NF110 alone (data not shown).

NF45 is relatively unstable and protected by NF90. We next examined the effect of NF90 depletion on the stability of NF45 protein, and vice versa. To determine the half-life of NF45, we conducted pulse-chase experiments in cells transfected with various siRNAs (Fig. 5B). NF45 was immunoprecipitated from cell extracts immediately after labeling or after 1 to 3 h of subsequent "chase" with unlabeled amino acids. As expected, no labeling of NF45 was detected in cells transfected with D5 siRNA. The half-life of NF45 was only 1.42 h, and it was further shortened by D2 and D3 siRNA to 0.53 h and 0.37 h, respectively (Fig. 5B). D4 siRNA elicited a smaller effect on the half-life of NF45, which was reduced to 0.95 h. Evidently, NF90 depletion accelerates NF45 turnover and NF110 deple-

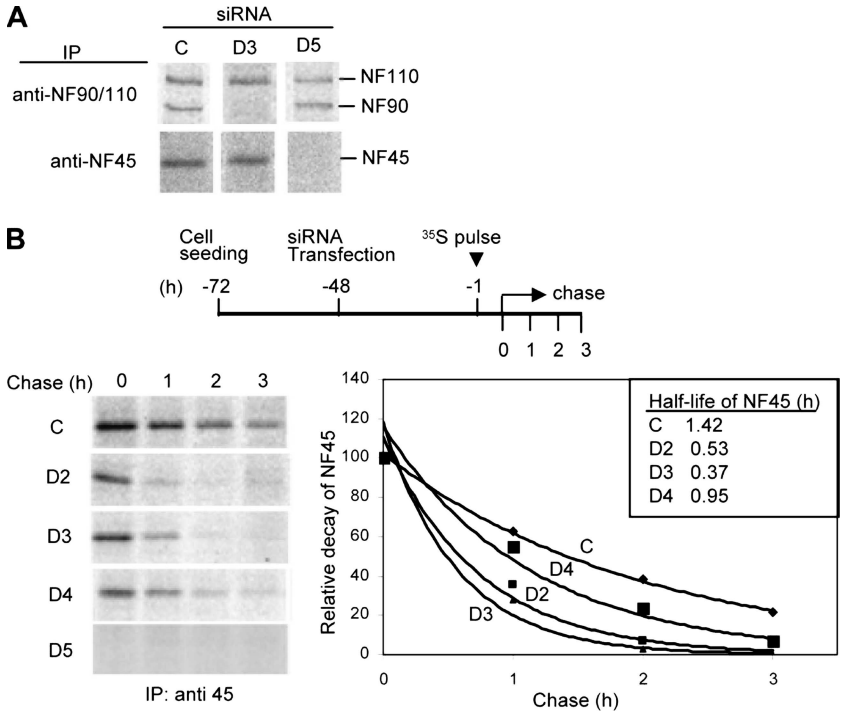

FIG. 5. NF90 depletion destabilizes NF45. (A) D3 and D5 siRNAs specifically reduce the synthesis of NF90 and NF45, respectively. HeLa cells transfected with C, D3, or D5 siRNA were labeled with [^{35}S]methionine for 1 h at 48 h posttransfection. Immunoprecipitates (IP) prepared with antibodies directed against NF90 and NF110 (upper panel) or NF45 (lower panel) were analyzed by gel electrophoresis and autoradiography. (B) Pulse-chase analysis of NF45 in cells transfected with C, D2, D3, D4, or D5 siRNA. Cells were labeled and chased as represented schematically in the diagram. NF45 was immunoprecipitated and detected as in panel A (left panel) and quantified by PhosphorImager (right panel). NF45 half-life (inset) was calculated according to equations drawn from respective curves using the Excel 2003 TREND function.

tion also has an effect on NF45 stability, even though this did not register as a detectable decrease in NF45 level (Fig. 4A).

Comparable analyses of effects on the stability of NF90 and NF110 were precluded by the long half-lives of these proteins, estimated at 2.4 and 1.8 days, respectively, in HeLa cells (data not shown). Slow turnover rates (half-lives of ~5 and ~3 days) have also been reported for these proteins in HepG2 cells (55). Further experiments, using the inhibitor MG-132, indicate that NF45 is probably degraded by the proteasome (see Fig. S3 in the supplemental material). We conclude that NF45 is a short-lived protein that is stabilized by binding to its partners and speculate that one of its roles is to stabilize NF90 and NF110.

Cell division is slowed by knockdown of NF90 or NF45. Transfection of D2, D3, or D5 significantly reduced the growth rates of cell cultures in comparison with those of cells that were mock transfected or transfected with control siRNA (Fig. 6A). D4, which knocks down NF110 alone, had little or no effect. Similarly, the stable cell lines d2, d3, and d5 grew more slowly than the d4 or control cell lines (Fig. 6B). Hence, the expansion of cultures is slowed by the knockdown of endogenous NF90, NF90, and NF110 or NF45, indicating that coordinate reduction of NF45 and NF90 is associated with growth retardation. Correspondingly, rescue of NF45 by NF90c was accompanied by accelerated growth of the d3 cell line (Fig. 6C).

We considered two possible explanations for this apparent slowing of cell growth: (i) that cell death is more frequent in cells depleted of NF90 and NF45 or (ii) that such cells are blocked in the cell cycle. Cell viability was assessed by trypan blue exclusion: <2% of the cells were stained in each cell line, indicating that little necrotic or apoptotic cell death was taking place. Fluorescence-activated cell sorting (FACS) analysis of the cell lines confirmed that each cell line had a similar, low percentage of apoptotic cells, and no significant accumulation of cells was observed in any compartment of the cell cycle (Fig. 6D to F), arguing against a block in progression in the cell lines. On the other hand, the incorporation of [^{3}H]thymidine into DNA was reduced in cells transfected with or stably expressing D2, D3, or D5 (Fig. 6A and B, insets). Thus, slow growth correlated with inhibition of DNA synthesis. Anomalously, [^{3}H]thymidine uptake was increased by D4, although cell growth was marginally reduced. We conclude that the slow growth brought about by depletion of NF90 and NF45 is accompanied by reduced DNA synthesis but not by a cell cycle block.

Multinucleated cells arise when NF90 or NF45 is knocked down. The d3 and d5 lines displayed a markedly increased proportion of cells with polyploid DNA content (11.2% and 17% compared to 6.8% in control) (Fig. 6D to F). This population could include cell aggregates as well as multinucleated cells. However, microscopic examination revealed that depletion of NF90 and NF45 caused a striking accumulation of multinucleated cells. This phenomenon can be visualized in cells stained simultaneously with Hoechst dye for DNA and with antitubulin antibody (Fig. 7A). Multinucleated cells accounted for ~5% of the population in the d2 and d3 cell lines and as many as ~12% in the d5 line, compared to <1% in the

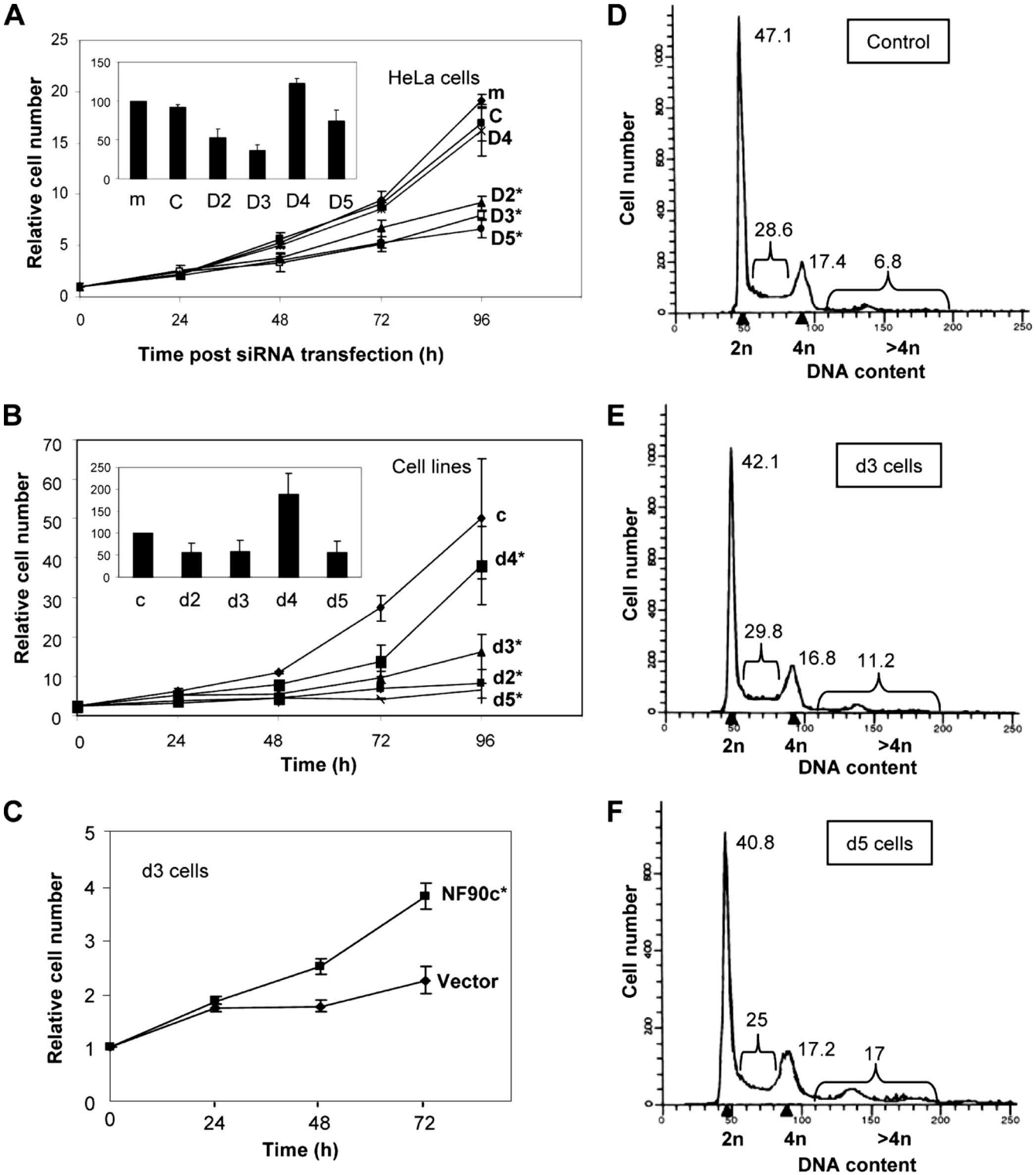

FIG. 6. Effects of NF45, NF90, and NF110 knockdown on cell growth. Cell growth curves were measured for cells described in the legend to Fig. 4. (A) HeLa cells mock transfected (m) or transfected with control (C), D2, D3, D4, or D5 siRNA. (B) Stable cell lines c, d2, d3, d4, and d5. (C) d3 cells transfected with pcDNA-NF90c. For [^{3}H]thymidine incorporation (insets), the average (control and mock values set at 100 U) and standard deviation were obtained from three experiments in triplicate. (D to F) Cell cycle analysis was performed on c, d3, and d5 cells stained with propidium iodide using a BD FACSCalibur cell sorter. The percentages of cells in the G_1, S, G_2/M, and polyploid compartments are indicated (left to right). *, $P < 0.01$ relative to controls at 48 h and all later time points (except for d4 at 48 h in panel B) by Student's *t* tests.

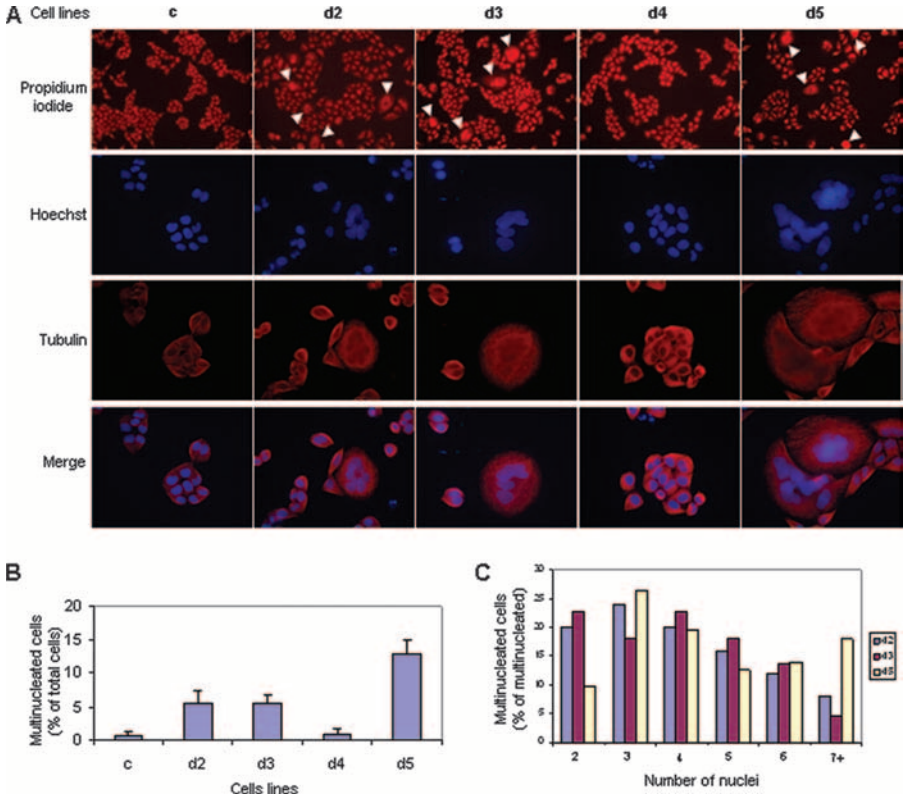

FIG. 7. Morphological changes in cell lines expressing shRNA. (A) Formation of multinucleated cells in d2, d3, and d5 cell lines. (Top panel) Cells stained with propidium iodide observed at low power (10 × 40). Multinucleated cells are indicated by arrowheads. (Lower panels) Cells stained with Hoechst 33342 and antitubulin antibody were observed at high magnification (10 × 60), and the images were merged. (B) Multinucleated cells were counted in three fields of 100 cells each. The percentage of such cells (with standard deviation) is plotted for each cell line. (C) The numbers of nuclei in multinucleated d2 cells (25 cells), d3 cells (22 cells), and d5 cells (72 cells) were counted. The percentage of multinucleated cells with a particular number of nuclei is plotted.

control and d4 lines (Fig. 7B). The number of nuclei per multinucleated cell ranged from 2 to 11 (Fig. 7C). Of the multinucleated d2 and d3 cells, the majority (>90%) had 2 to 6 nuclei. In d5 cells, however, over 15% had seven or more nuclei, indicating that NF45 depletion results in a more severe phenotype. The rare multinucleated cells in control and d2 cultures usually had only two nuclei per cell (data not shown).

To verify that the multiple nuclei lie within the same cell, we conducted photobleaching experiments. Bleaching within a small localized area of the cytoplasm of a multinucleated d5 cell led to the loss in fluorescence of all of the cytoplasm of the multinucleated cell, whereas adjacent cells were unaffected (Fig. 8A). Observation under the fluorescent microscope suggested that the multiple nuclei were often connected as visualized in serial z-sections of live cells expressing fluorescent histone-CFP (Fig. 8B). Thus the cells are not true syncytia. These observations suggest that NF90 and NF45 are required for the final stages of nuclear separation and cytokinesis during mitosis.

DISCUSSION

Structure of NF90/110 complexes with NF45. NF90 and NF110 occur in complexes with NF45 and several other proteins in many cells. In accord with published observations (27), we did not detect monomeric NF90 or NF45 in the nucleus or cytoplasm. Our hydrodynamic data show that the core complexes obtained from cells after RNase treatment are heterodimeric: NF90-NF45 and NF110-NF45. Native complexes are much larger because of association with both RNA and protein components. They are stable under conditions of gel filtration and immunoprecipitation but labile, for reasons that are unclear, to sedimentation through glycerol gradients. The composition of these large complexes is not yet fully defined, although many of their components are known. Several RNAs, both small noncoding RNAs and mRNAs, have been found in complexes with NF90. The RNase sensitivity of the large complexes implies that RNA molecules contribute to the stability of higher-order complexes, consistent with the RNA-mediated interaction of ADAR1 with NF90, NF110, and NF45 (28) and with our finding of ADAR1 and the DDX3X helicase in complexes from untreated but not RNase-treated extracts. Several proteins have been reported to associate with NF90/110, and additional partners are reported here. In keeping with the involvement of NF90/110 in RNA metabolism, these include two further RNA helicases, nucleolin, and several hnRNP proteins. The presence in NF90 complexes of matrin-3 with structural roles in the cell may be correlated with the newly discovered function of NF90 and NF45 in mitosis.

The higher-order complexes are likely to be heterogeneous

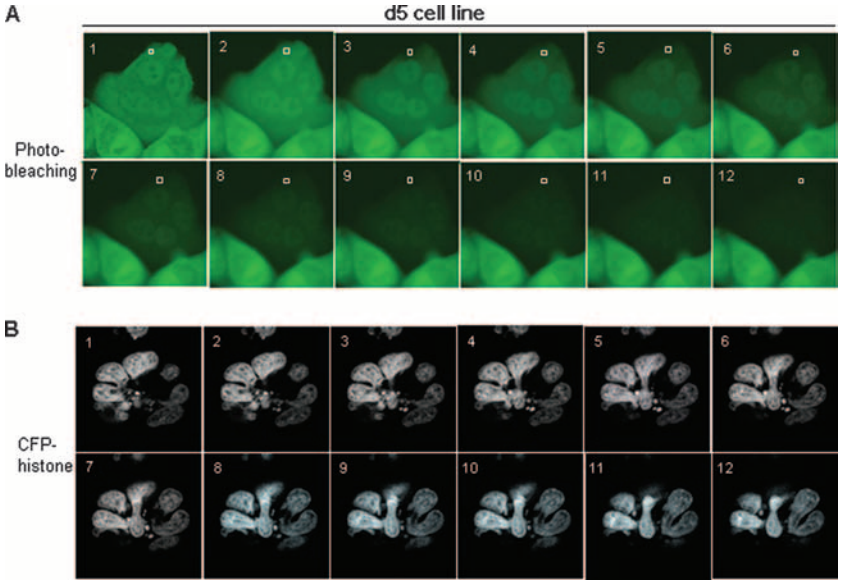

FIG. 8. Interconnected nuclei in d5 cells. (A) Photobleaching of a multinucleated d5 cell. An individual cell in a d5 culture transfected with GFP was repeatedly bleached over a short period of time by a laser beam directed at the square indicated in the cytoplasm. Shown are images taken at 15-s intervals. Note that fluorescence in the neighboring cells was undiminished, whereas all the nuclei in the targeted cell were bleached. (B) Confocal microscopy of a living d5 cells transfected with histone-CFP. Serial pictures were taken from the bottom to the top of the cell: images taken at 0.5-μm intervals are shown.

in composition, and they also appear to be cell-type specific (27). Coimmunoprecipitation evidence supported by reconstitution experiments demonstrates the existence of complexes containing two or more molecules of NF90/110. Interactions between molecules of NF90/110 in vitro are mediated by the dsRBMs but do not require RNA. We therefore speculate that the dsRBMs participate in NF90/110 dimer formation and in interactions with RNA but not both at the same time. NF45 binding is thought to activate NF90 by a structural change that relieves autoinhibition by its N terminus (38). It is possible that this regulation is mediated by an effect of NF45 on the ability of NF90 to dimerize or interact with its RNA and protein partners.

The physiological relevance of the NF90-NF45 and NF110-NF45 core complexes is demonstrated by the mutual stabilization of their heterodimeric components. Knockdown of NF90 destabilized NF45, and vice versa. Similarly, NF110 and NF45 are coregulated. Although NF45 levels were not discernibly reduced when NF110 was depleted, the half-life of NF45 was somewhat shortened. The reason for the different behavior is not immediately obvious but could be related to the larger amount of NF90 in the cell relative to NF110 (33). Coregulation of protein partners has been observed in other cases, such as the P-TEFb (9) and survivin–caspase-3–$p21^{WAF1/CIP1}$ complexes (7, 21), and it may be an important mechanism evolved to allow for prompt reaction to environmental changes.

Roles of NF90/110 complexes with NF45. The components of the core complexes have remarkably different stabilities and, hence, rates of synthesis. In HeLa cells, the half-lives of NF90 and NF110 (about 2.4 and 1.8 days, respectively) are over 30 times longer than that of NF45 (1.4 h). This rapid turnover makes NF45 well suited for a role as a regulatory subunit. Deletions within its DZF region impair binding to NF90, but deletion of the N-terminal RGG region is tolerated (data not shown). The DZF motif is present in several proteins that are important for cell proliferation and development (11, 24). NF90 and NF110 both have several functional motifs associated with nucleic acid binding and nuclear localization signals as well as an RGG motif. Our results show that the N-terminal region aa 1 to 591 of NF90/110, which includes the DZF domain, is fully functional in stabilizing NF45 and rescuing cell growth caused by the destruction of NF90-NF45 complexes. However, we do not know if the dsRBMs are necessary for cell growth.

Both NF90 and NF45 are widely distributed in human organs (43, 56), implying pivotal roles in many types of cell. NF90 is phosphorylated in M phase, suggestive of a function in cell division (23). In *Xenopus*, the NF110 homologue, $CBTF^{122}$, is thought to be important for transcription of the zygotic genome (4). Overexpression of NF90 was observed in malignant human nasopharyngeal carcinoma cells (13), but does not result in faster growth of 293 cells in tissue culture (our unpublished observations). In mice, *ILF3* gene knockout resulted in underdevelopment of muscle, causing respiratory failure and death (44). These observations suggested an involvement of NF90/110 in cell growth, consistent with our finding that knockdown of endogenous NF90 or NF45 retards cell growth in HeLa cells. Slowed cell growth is possibly a result of decreased DNA synthesis, but intriguingly no blockage of the cell cycle was observed. Faster apoptosis and cell death in NF45- or NF90-depleted cells were excluded by FACS and live-cell counting.

Despite their extensive sequence overlap and strong similarities, NF110 exhibits functional differences from NF90. NF110 knockdown had only a minor effect on NF45 levels and on cell growth, did not lead to the formation of multinucleated cells,

and increased rather than decreased DNA synthesis in HeLa cells. NF110 is more tightly associated with the nucleus than NF90 (33), and NF90, but not NF110, moves from the nucleus to the cytoplasm in activated Jurkat cells (27). NF110 isoforms are more active than NF90 isoforms in stimulating transcription from the proliferating cell nuclear antigen promoter in a transient expression system (10) and NF110 interacts with the protein methylase PRMT1 (49). Unlike NF90, NF110 does not bind the human rhinovirus type 2 internal ribosome entry site (26). NF110 is almost entirely restricted to the nucleus, and it is possible that it exerts an opposite function from that of NF90 in this compartment via its differential interactions with other cellular components.

Formation of multinucleated cells. Depletion of NF45 or, to a lesser extent, of NF90 leads to a mitotic defect resulting in the accumulation of multinucleated cells. Many of the nuclei remain connected to one another, suggesting a defect in cytokinesis. Large nuclei and greater numbers of multinucleated giant-fusing myocytes were observed in NF90-deficient mice (44). However, these findings were interpreted as suggesting that skeletal muscle development is delayed in the NF90 knockout mice or that their muscle fibers undergo degeneration and regeneration. Accumulation of multinucleated HeLa cells has been reported after depletion of components of the chromosomal passenger complex, including survivin, EVI5, and aurora, or of ORC6, a component of the origin recognition complex. For example, survivin-depleted cells were delayed in mitosis and failed in cytokinesis, possibly because of dysfunction of microtubule bundles that formed the midbody (7, 21, 51). Silencing of ORC6 expression by siRNA resulted in cells with multipolar spindles, aberrant mitosis, formation of multinucleated cells, and decreased DNA replication (8, 35).

Previous studies noted the migration of NF90, NF110, and NF45 from the nucleus into the cytoplasm during mitosis (2, 23, 33, 50). This release appears to be due to the weakening of protein-protein interactions that tether NF90 and NF110 in the interphase nucleus as a result of their phosphorylation (33). The translocation of the proteins implied a relationship with mitosis but did not disclose its nature or whether they have a functional role in mitosis as demonstrated here. While our data do not clearly distinguish between direct and indirect effects of NF90-NF45, the latter seems more likely based on the properties of the proteins known to date. Furthermore, even though NF90, NF110, and NF45 are all associated with chromatin, NF110 is more tightly bound than NF90 (39), yet NF110 depletion did not cause the appearance of multinucleated cells. Indirect effects could be mediated through protein-protein or protein-RNA interactions. NF90 binds to the mRNA encoding Tau, a tubulin-binding protein required for microtubule assembly and cytokinesis (6, 20, 54), but we did not observe changes of tubulin level when NF90/110 and NF45 were depleted. Another possibility takes note of the action of NF90 and NF45 to increase DNA binding by the Ku regulatory subunits of DNA-PK, suggesting an involvement in DNA repair and chromosome stability (2, 50). Cells deficient in DNA-PK accumulated telomeric fusions and anaphase bridges during mitosis (15). Consistent with a role in the synthesis or stability of components required for cytokinesis, NF90 is associated with matrin-3, which participates in cell architecture and dynamics. On the other hand, there are many NF90-RNA interactions that could have implications for mitosis. For example, NF90 stabilizes the mRNA for $p21^{WAF1/CIP1}$ (44), a protein that is associated with survivin (7, 21). This observation suggests another attractive explanation for the genesis of multinucleated cells, in which NF90-NF45 knockdown results in depletion of the survivin-caspase-p21 complex. Further work is needed to test these models and to establish the mechanisms whereby NF90/110 and NF45 affect DNA synthesis, cytokinesis, and cell growth.

ACKNOWLEDGMENTS

We thank D. Stein for flow cytometry analysis and M. Hoque and R. Shammana for helpful discussions.

This work was supported by grant AI34552 to M.B.M. and by fellowship GM069139 to C.J.A. from the National Institutes of Health.

REFERENCES

1. **Altan-Bonnet, N., R. D. Phair, R. S. Polishchuk, R. Weigert, and J. Lippincott-Schwartz.** 2003. A role for Arf1 in mitotic Golgi disassembly, chromosome segregation, and cytokinesis. Proc. Natl. Acad. Sci. USA **100:**13314–13319.
2. **Aoki, Y., G. Zhao, D. Qiu, L. Shi, and P. N. Kao.** 1998. CsA-sensitive purine-box transcriptional regulator in bronchial epithelial cells contains NF45, NF90, and Ku. Am. J. Physiol. **275:**L1164–L1172.
3. **Bass, B. L., S. R. Hurst, and J. D. Singer.** 1994. Binding properties of newly identified Xenopus proteins containing dsRNA-binding motifs. Curr. Biol. **4:**301–316.
4. **Brzostowski, J., C. Robinson, R. Orford, S. Elgar, G. Scarlett, T. Peterkin, M. Malartre, G. Kneale, M. Wormington, and M. Guille.** 2000. RNA-dependent cytoplasmic anchoring of a transcription factor subunit during Xenopus development. EMBO J. **19:**3683–3693.
5. **Burckstummer, T., K. L. Bennett, A. Preradovic, G. Schutze, O. Hantschel, G. Superti-Furga, and A. Bauch.** 2006. An efficient tandem affinity purification procedure for interaction proteomics in mammalian cells. Nat. Methods **3:**1013–1019.
6. **Chau, M. F., M. J. Radeke, C. de Ines, I. Barasoain, L. A. Kohlstaedt, and S. C. Feinstein.** 1998. The microtubule-associated protein tau cross-links to two distinct sites on each alpha and beta tubulin monomer via separate domains. Biochemistry **37:**17692–17703.
7. **Chen, J., W. Wu, S. K. Tahir, P. E. Kroeger, S. H. Rosenberg, L. M. Cowsert, F. Bennett, S. Krajewski, M. Krajewska, K. Welsh, J. C. Reed, and S. C. Ng.** 2000. Down-regulation of survivin by antisense oligonucleotides increases apoptosis, inhibits cytokinesis and anchorage-independent growth. Neoplasia **2:**235–241.
8. **Chesnokov, I. N., O. N. Chesnokova, and M. Botchan.** 2003. A cytokinetic function of Drosophila ORC6 protein resides in a domain distinct from its replication activity. Proc. Natl. Acad. Sci. USA **100:**9150–9155.
9. **Chiu, Y.-L., H. Cao, J.-M. Jacque, M. Stevenson, and T. M. Rana.** 2004. Inhibition of human immunodeficiency virus type 1 replication by RNA interference directed against human transcription elongation factor P-TEFb (CDK9/cyclinT1). J. Virol. **78:**2517–2529.
10. **Corthésy, B., and P. N. Kao.** 1994. Purification by DNA affinity chromatography of two polypeptides that contact the NF-AT DNA binding site in the interleukin 2 promoter. J. Biol. Chem. **269:**20682–20690.
11. **Doran, B., N. Gherbesi, G. Hendricks, R. A. Flavell, R. J. Davis, and L. Gangwani.** 2006. Deficiency of the zinc finger protein ZPR1 causes neurodegeneration. Proc. Natl. Acad. Sci. USA **103:**7471–7475.
12. **Duchange, N., J. Pidoux, E. Camus, and D. Sauvaget.** 2000. Alternative splicing in the human interleukin enhancer binding factor 3 (ILF3) gene. Gene **261:**345–353.
13. **Fung, L. F., A. K. Lo, P. W. Yuen, Y. Liu, X. H. Wang, and S. W. Tsao.** 2000. Differential gene expression in nasopharyngeal carcinoma cells. Life Sci. **67:**923–936.
14. **Furmaniak, J., E. D. Jones, P. R. Buckland, R. D. Howells, and B. R. Smith.** 1986. Assessment of the shape and molecular size of TSH-TSH receptor complexes. Mol. Cell. Endocrinol. **48:**31–38.
15. **Goytisolo, F. A., E. Samper, S. Edmonson, G. E. Taccioli, and M. A. Blasco.** 2001. The absence of the DNA-dependent protein kinase catalytic subunit in mice results in anaphase bridges and in increased telomeric fusions with normal telomere length and G-strand overhang. Mol. Cell. Biol. **21:**3642–3651.
16. **Isken, O., C. W. Grassmann, R. T. Sarisky, M. Kann, S. Zhang, F. Grosse, P. N. Kao, and S.-E. Behrens.** 2003. Members of the NF90/NFAR protein group are involved in the life cycle of a positive-strand RNA virus. EMBO J. **22:**5655–5665.
17. **Kao, P. N., L. Chen, G. Brock, J. Ng, J. Kenny, A. J. Smith, and B. Corthésy.** 1994. Cloning and expression of cyclosporin A- and FK506-sensitive nuclear factor of activated T-cells: NF45 and NF90. J. Biol. Chem. **269:**20691–20699.

18. **Krasnoselskaya-Riz, I., A. Spruill, Y. W. Chen, D. Schuster, T. Teslovich, C. Baker, A. Kumar, and D. A. Stephan.** 2002. Nuclear factor 90 mediates activation of the cellular antiviral expression cascade. AIDS Res. Hum. Retrovir. **18:**591–604.
19. **Langland, J. O., P. N. Kao, and B. L. Jacobs.** 1999. Nuclear factor-90 of activated T-cells: a double-stranded RNA-binding protein and substrate for the double-stranded RNA-dependent protein kinase, PKR. Biochemistry **38:**6361–6368.
20. **Larcher, J. C., L. Gasmi, W. Viranaicken, B. Edde, R. Bernard, I. Ginzburg, and P. Denoulet.** 2004. Ilf3 and NF90 associate with the axonal targeting element of Tau mRNA. FASEB J. **18:**1761–1763.
21. **Li, F., E. J. Ackermann, C. F. Bennett, A. L. Rothermel, J. Plescia, S. Tognin, A. Villa, P. C. Marchisio, and D. C. Altieri.** 1999. Pleiotropic cell-division defects and apoptosis induced by interference with survivin function. Nat. Cell Biol. **1:**461–466.
22. **Liao, H. J., R. Kobayashi, and M. B. Mathews.** 1998. Activities of adenovirus virus-associated RNAs: purification and characterization of RNA binding proteins. Proc. Natl. Acad. Sci. USA **95:**8514–8519.
23. **Matsumoto-Taniura, N., F. Pirollet, R. Monroe, L. Gerace, and J. M. Westendorf.** 1996. Identification of novel M phase phosphoproteins by expression cloning. Mol. Biol. Cell **7:**1455–1469.
24. **Meagher, M. J., and R. E. Braun.** 2001. Requirement for the murine zinc finger protein ZFR in perigastrulation growth and survival. Mol. Cell. Biol. **21:**2880–2890.
25. **Meagher, M. J., J. M. Schumacher, K. Lee, R. W. Holdcraft, S. Edelhoff, C. Disteche, and R. E. Braun.** 1999. Identification of ZFR, an ancient and highly conserved murine chromosome-associated zinc finger protein. Gene **228:**197–211.
26. **Merrill, M. K., E. Y. Dobrikova, and M. Gromeier.** 2006. Cell-type-specific repression of internal ribosome entry site activity by double-stranded RNA-binding protein 76. J. Virol. **80:**3147–3156.
27. **Merrill, M. K., and M. Gromeier.** 2006. The double-stranded RNA binding protein 76:NF45 heterodimer inhibits translation initiation at the rhinovirus type 2 internal ribosome entry site. J. Virol. **80:**6936–6942.
28. **Nie, Y., L. Ding, P. N. Kao, R. Braun, and J.-H. Yang.** 2005. ADAR1 interacts with NF90 through double-stranded RNA and regulates NF90-mediated gene expression independently of RNA editing. Mol. Cell. Biol. **25:**6956–6963.
29. **Parker, L. M., I. Fierro-Monti, and M. B. Mathews.** 2001. Nuclear factor 90 is a substrate and regulator of the eukaryotic initiation factor 2 kinase double-stranded RNA-activated protein kinase. J. Biol. Chem. **276:**32522–32530.
30. **Parker, L. M., I. Fierro-Monti, T. W. Reichman, S. Gunnery, and M. B. Mathews.** 2001. Double-stranded RNA-binding proteins and the control of protein synthesis and cell growth. Cold Spring Harb. Symp. Quant. Biol. **66:**485–497.
31. **Parrott, A. M., and M. B. Mathews.** 2007. Novel rapidly evolving hominid RNAs bind nuclear factor 90 and display tissue-restricted distribution. Nucleic Acids Res. **35:**6249–6258.
32. **Parrott, A. M., M. R. Walsh, and M. B. Mathews.** 2007. Analysis of RNA: protein interactions in vivo: identification of RNA binding partners of nuclear factor 90. Methods Enzymol. **429:**243–260.
33. **Parrott, A. M., M. R. Walsh, T. W. Reichman, and M. B. Mathews.** 2005. RNA binding and phosphorylation determine the intracellular distribution of nuclear factors 90 and 110. J. Mol. Biol. **348:**281–293.
34. **Patel, R. C., D. J. Vestal, Z. Xu, S. Bandyopadhyay, W. Guo, S. M. Erme, B. R. Williams, and G. C. Sen.** 1999. DRBP76, a double-stranded RNA-binding nuclear protein, is phosphorylated by the interferon-induced protein kinase, PKR. J. Biol. Chem. **274:**20432–20437.
35. **Prasanth, S. G., K. V. Prasanth, and B. Stillman.** 2002. Orc6 involved in DNA replication, chromosome segregation, and cytokinesis. Science **297:**1026–1031.
36. **Ranpura, S. A., U. S. Deshmukh, and P. P. Reddi.** 2007. NF45 and NF90 in murine seminiferous epithelium: potential role in SP-10 gene transcription. J. Androl. **29:**186–197.
37. **Reichman, T. W., and M. B. Mathews.** 2003. RNA binding and intramolecular interactions modulate the regulation of gene expression by nuclear factor 110. RNA **9:**543–554.
38. **Reichman, T. W., L. C. Muñiz, and M. B. Mathews.** 2002. The RNA binding protein nuclear factor 90 functions as both a positive and negative regulator of gene expression in mammalian cells. Mol. Cell. Biol. **22:**343–356.
39. **Reichman, T. W., A. M. Parrott, I. Fierro-Monti, D. J. Caron, P. N. Kao, C. G. Lee, H. Li, and M. B. Mathews.** 2003. Selective regulation of gene expression by nuclear factor 110, a member of the NF90 family of double-stranded RNA-binding proteins. J. Mol. Biol. **332:**85–98.
40. **Sakamoto, S., K. Morisawa, K. Ota, J. Nie, and T. Taniguchi.** 1999. A binding protein to the DNase I hypersensitive site II in HLA-DR alpha gene was identified as NF90. Biochemistry **38:**3355–3361.
41. **Satoh, M., V. M. Shaheen, P. N. Kao, T. Okano, M. Shaw, H. Yoshida, H. B. Richards, and W. H. Reeves.** 1999. Autoantibodies define a family of proteins with conserved double-stranded RNA-binding domains as well as DNA binding activity. J. Biol. Chem. **274:**34598–34604.
42. **Saunders, L. R., V. Jurecic, and G. N. Barber.** 2001. The 90- and 110-kDa human NFAR proteins are translated from two differentially spliced mRNAs encoded on chromosome 19p13. Genomics **71:**256–259.
43. **Saunders, L. R., D. J. Perkins, S. Balachandran, R. Michaels, R. Ford, A. Mayeda, and G. N. Barber.** 2001. Characterization of two evolutionarily conserved, alternatively spliced nuclear phosphoproteins, NFAR-1 and -2, that function in mRNA processing and interact with the double-stranded RNA-dependent protein kinase, PKR. J. Biol. Chem. **276:**32300–32312.
44. **Shi, L., G. Zhao, D. Qiu, W. R. Godfrey, H. Vogel, T. A. Rando, H. Hu, and P. N. Kao.** 2005. NF90 regulates cell cycle exit and terminal myogenic differentiation by direct binding to the 3′-untranslated region of MyoD and p21WAF1/CIP1 mRNAs. J. Biol. Chem. **280:**18981–18989.
45. **Shim, J., H. Lim, J. R. Yates, and M. Karin.** 2002. Nuclear export of NF90 is required for interleukin-2 mRNA stabilization. Mol. Cell **10:**1331–1344.
46. **Shin, H. J., S. S. Kim, Y. H. Cho, S. G. Lee, and H. M. Rho.** 2002. Host cell proteins binding to the encapsidation signal epsilon in hepatitis B virus RNA. Arch. Virol. **147:**471–491.
47. **Siegel, L. M., and K. J. Monty.** 1966. Determination of molecular weights and frictional ratios of proteins in impure systems by use of gel filtration and density gradient centrifugation. Application to crude preparations of sulfite and hydroxylamine reductases. Biochim. Biophys. Acta **112:**346–362.
48. **Sui, G., C. Soohoo, E. B. Affar, F. Gay, Y. Shi, and W. C. Forrester.** 2002. A DNA vector-based RNAi technology to suppress gene expression in mammalian cells. Proc. Natl. Acad. Sci. USA **99:**5515–5520.
49. **Tang, J., P. N. Kao, and H. R. Herschman.** 2000. Protein-arginine methyltransferase I, the predominant protein-arginine methyltransferase in cells, interacts with and is regulated by interleukin enhancer-binding factor 3. J. Biol. Chem. **275:**19866–19876.
50. **Ting, N. S., P. N. Kao, D. W. Chan, L. G. Lintott, and S. P. Lees-Miller.** 1998. DNA-dependent protein kinase interacts with antigen receptor response element binding proteins NF90 and NF45. J. Biol. Chem. **273:**2136–2145.
51. **Uren, A. G., L. Wong, M. Pakusch, K. J. Fowler, F. J. Burrows, D. L. Vaux, and K. H. Choo.** 2000. Survivin and the inner centromere protein INCENP show similar cell-cycle localization and gene knockout phenotype. Curr. Biol. **10:**1319–1328.
52. **Van Herreweghe, E., S. Egloff, I. Goiffon, B. E. Jady, C. Froment, B. Monsarrat, and T. Kiss.** 2007. Dynamic remodelling of human 7SK snRNP controls the nuclear level of active P-TEFb. EMBO J. **26:**3570–3580.
53. **Viranaicken, W., L. Gasmi, C. Chauvin, P. Denoulet, and J. C. Larcher.** 2006. Identification of a newly spliced exon in the mouse Ilf3 gene generating two long and short isoforms of Ilf3 and NF90. Genomics **88:**622–632.
54. **Weingarten, M. D., A. H. Lockwood, S. Y. Hwo, and M. W. Kirschner.** 1975. A protein factor essential for microtubule assembly. Proc. Natl. Acad. Sci. USA **72:**1858–1862.
55. **Xu, Y. H., T. Leonova, and G. A. Grabowski.** 2003. Cell cycle dependent intracellular distribution of two spliced isoforms of TCP/ILF3 proteins. Mol. Genet. Metab. **80:**426–436.
56. **Zhao, G., L. Shi, D. Qiu, H. Hu, and P. N. Kao.** 2005. NF45/ILF2 tissue expression, promoter analysis, and interleukin-2 transactivating function. Exp. Cell Res. **305:**312–323.